Acta Crystallographica Section A
Foundations of Crystallography
ISSN 0108-7673

Received 25 August 2009
Accepted 3 December 2009

Ultrafast X-ray diffraction in liquid, solution and gas: present status and future prospects

Jeongho Kim, Kyung Hwan Kim, Jae Hyuk Lee and Hyotcherl Ihee*

Center for Time-Resolved Diffraction, Department of Chemistry, and Graduate School of Nanoscience and Technology (WCU), KAIST, Daejeon 305-701, Republic of Korea. Correspondence e-mail: hyotcherl.ihee@kaist.ac.kr

In recent years, the time-resolved X-ray diffraction technique has been established as an excellent tool for studying reaction dynamics and protein structural transitions with the aid of 100 ps X-ray pulses generated from third-generation synchrotrons. The forthcoming advent of the X-ray free-electron laser (XFEL) will bring a substantial improvement in pulse duration, photon flux and coherence of X-ray pulses, making time-resolved X-ray diffraction even more powerful. This technical breakthrough is envisioned to revolutionize the field of reaction dynamics associated with time-resolved diffraction methods. Examples of candidates for the first femtosecond X-ray diffraction experiments using highly coherent sub-100 fs pulses generated from XFELs are presented in this paper. They include the chemical reactions of small molecules in the gas and solution phases, solvation dynamics and protein structural transitions. In these potential experiments, ultrafast reaction dynamics and motions of coherent rovibrational wave packets will be monitored in real time. In addition, high photon flux and coherence of XFEL-generated X-ray pulses give the prospect of single-molecule diffraction experiments.

1. Introduction

The focus of investigation in the field of reaction dynamics is to develop a molecular-level understanding of how a chemical reaction proceeds from reactants to products by the motions of constituent atoms in reacting molecules. Over several decades, researchers in the field have made many efforts to probe the molecular motions involved in the chemical reactions occurring in gas and condensed phases by developing novel spectroscopic tools to measure such changes. However, despite all the advances of spectroscopic tools for studying reaction dynamics, it still remains quite challenging to investigate the detailed motions involved in chemical reactions, even for elementary reactions.

Reaction dynamics in gas and solution phases have been traditionally studied by time-resolved pump–probe spectroscopy that commonly employs coherent femtosecond optical pulses (Khundkar & Zewail, 1990; Zewail, 1994; Hertel & Radloff, 2006). In typical pump–probe spectroscopy implemented in the optical regime, a reaction is initiated by an optical laser pulse (pump) and the progress of the reaction is monitored by another optical pulse (probe) as a function of the time delay between the pump and probe pulses. Mapping the pump–probe signals as a function of time delays between the pulses can reveal useful information such as the lifetime of an energy state and vibrational wave packet motions along potential energy surfaces. The time-resolved pump–probe spectroscopy can be extended by replacing the optical probe pulse by a different type of probe so that richer dynamical information can be obtained. For example, the reactions in the gas phase can be efficiently probed by ion detection using mass spectrometry because of its high sensitivity to even a small amount of chemical species (Johnson & Otis, 1981). Also, photoelectrons can be used as a sensitive probe of the dynamics of molecules and clusters (Neumark, 2001; Stolow, 2003), especially becoming more powerful when combined with ion-imaging techniques that allow simultaneous measurement of rotational, vibrational, electronic and translational energy distributions of products (Chandler & Houston, 1987; Heck & Chandler, 1995). For reactions in the liquid and solution phases, time-resolved transient absorption and fluorescence spectroscopy at the UV and visible frequencies have been the most popular choice owing to simplicity in their implementation and high sensitivity to specific electronic states (Fleming, 1986; Kao *et al.*, 2005; Qiu *et al.*, 2007; Zhang *et al.*, 2007). Besides, time-resolved vibrational spectroscopies that make use of infrared pulses or the Raman process have been used to study reaction dynamics in liquid and solution owing to the rather direct connection of vibrational transition frequencies with molecular structure (Nibbering *et al.*, 2005; Kukura *et al.*, 2007).

The limitation of optical pump–probe spectroscopy is that the spectroscopic signals are sensitive to only specific energy states or chromophores, and thus are not directly related to the global structure of the molecules at the atomic level, for example, atomic coordinates, bond lengths and bond angles.

This limitation of the optical spectroscopy can be complemented by using X-ray pulses as probes. In contrast to visible or infrared light that probes electronic or vibrational transitions of specific chromophores, X-rays are diffracted (or scattered) off all atom–atom pairs and chemical species present in the molecule, thus direct information on the molecular structure can be retrieved from the measured X-ray diffraction patterns. Taking advantage of such high sensitivity of X-rays to atomic-level molecular structure, time-resolved X-ray diffraction (or scattering) techniques have been applied to study the structural dynamics of chemical reactions.

Thus far, compared with optical spectroscopy, the major limitation of the time-resolved X-ray diffraction technique has originated from the limited temporal duration of the X-ray pulses available, at best $\sim$100 ps from third-generation synchrotrons. Although laser-driven plasma or accelerator-based femtosecond X-ray sources have been previously applied to study the dynamics of phonons, heating and phase transitions in simple solid systems (Rischel *et al.*, 1997; Cavalleri *et al.*, 2005, 2006; Bargheer *et al.*, 2006), their low photon flux prevents us from keeping track of structural changes occurring in more complex systems such as polyatomic molecules and proteins. Now, this limitation can be overcome with the advent of novel sources of generating ultrashort X-ray pulses. One of them is the X-ray free-electron laser (XFEL), using self-amplified spontaneous emission from a linear electron accelerator. The XFEL can generate highly coherent, sub-100 fs X-ray pulses with high photon flux and will be operational starting from the year 2010. This technical breakthrough in X-ray pulse generation technology is expected to revolutionize ultrafast X-ray science, opening many great opportunities for developing novel experiments and theories. The aim of this paper is to propose the potential applications of the XFEL to studying reaction dynamics by taking full advantage of the highly coherent nature of ultrashort X-ray pulses generated from the XFEL.

2. Comparison of time-resolved X-ray diffraction and electron diffraction

To explore the vast potential of applying the XFEL to the study of reaction dynamics, it would be worthwhile to compare two representative methods based on diffraction phenomena: time-resolved electron diffraction (TRED) and time-resolved X-ray diffraction (TRXD) techniques. The two different but closely related techniques have been successful in investigating reaction dynamics by making use of the direct relationship of the diffraction pattern of electrons or X-rays with the global molecular structure. The two techniques are common in that they use a photoinitiation (pump) laser pulse to clock the chemical reaction and the induced changes are subsequently probed by another (probe) pulse. On the other hand, they use different types of probe pulses that have their own advantages and limitations (Pirenne, 1946; Shorokhov *et al.*, 2005; Chergui & Zewail, 2009), which will be discussed in this section. The lessons learned from the advance of these two techniques will give insight to the future applications of time-resolved X-ray diffraction using XFELs.

Fig. 1 schematically summarizes the applications of the TRXD and TRED techniques depending on the type of sample and achieved timescale. Electrons have a higher scattering intensity by five to six orders of magnitude than X-rays, and thus have a lower penetration depth than X-rays (Pirenne, 1946; Hargittai & Hargittai, 1988). These properties of electrons make TRED better suited for studying structural dynamics in the gas phase (Williamson *et al.*, 1997; Ihee *et al.*, 2001; Ruan *et al.*, 2001), in thin films (Siwick *et al.*, 2003; Cao *et al.*, 2003; Gedik *et al.*, 2007; Baum *et al.*, 2007; Sciaini *et al.*, 2009) and at the surface (Ruan *et al.*, 2004; Yang & Zewail, 2009). In addition, TRED has the advantage of simplicity in implementation over TRXD because electron pulses can be readily manipulated in a compact unit for a table-top experiment in contrast to X-ray pulses commonly requiring a huge synchrotron facility for generation of high-flux pulses. However, electrons are charged and hence easily affected by small amounts of positive ions generated as by-products in most pump–probe experiments. This sensitive nature of electrons causes baseline drift and complication of the data analysis (Ihee *et al.*, 2002).

In turn, the penetration depth of X-rays is higher than that of electrons, making it easier to apply the TRXD to condensed phase samples such as solid crystals, liquid solutions, proteins and nanoclusters (Perman *et al.*, 1998; Collet *et al.*, 2003; Coppens *et al.*, 2004; Ihee *et al.*, 2005*a*,*b*; Kotaidis & Plech, 2005; Davidsson *et al.*, 2005; Kim *et al.*, 2006; Plech *et al.*, 2006; Ihee, 2009; Vorontsov *et al.*, 2009; Christensen *et al.*, 2009), which are not accessible with electron diffraction (Fig. 1). This feature of TRXD is greatly beneficial for studying reaction dynamics since many of the important chemical reactions in chemistry and biology occur in condensed phases. The major limitation of TRXD arises from inelastic scattering that increases with the scattering angle. As a result, the signal-to-noise ratio for the elastic scattering signal at high q values

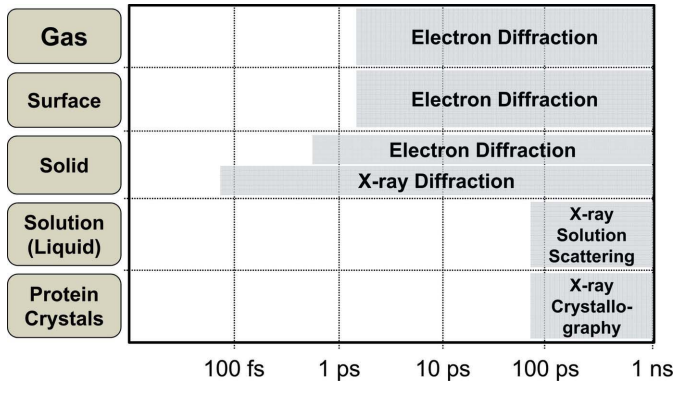

Figure 1
Present status of time-resolved X-ray and electron diffraction techniques in their applications to studying dynamics in various phases and timescales. Thus far, the low penetration depth of electron diffraction has limited its application to only the gas phase, surface and thin films. In contrast, the X-ray diffraction technique has been applied to even (liquid) solution-phase and protein crystals, but its relatively poor time resolution has been a major limitation.

deteriorates owing to the inelastic scattering serving as noise, even with a high flux of incoming X-ray photons. In contrast, the available q-range of electron diffraction is only limited by the magnitude of the electron flux. Besides, TRXD is not sensitive to hydrogen atoms, so it is not easy to track changes in the hydrogen coordinates during a chemical transition. Although this property might be considered a disadvantage compared with electron diffraction, it turns out to be advantageous in some cases. For example, when the experimental data are fitted by a model for molecular structure, the absence of hydrogen contributions to the signal greatly reduces the number of fitting parameters, simplifying the analysis.

Besides the differences described above, the most notable difference between the two techniques in the reaction dynamics studies has been the time resolution. TRXD can achieve $\sim$100 ps time resolution by using X-ray pulses from a synchrotron. In turn, TRED can achieve a time resolution down to $\sim$1 ps, which is about two orders of magnitude better than the time resolution of TRXD. However, the picosecond time resolution of TRED is still relatively poor compared with that of optical spectroscopy (tens of femtoseconds) as well as the timescale of many important molecular processes in chemical and biological systems. Therefore, only limited dynamics could be measured on the ultrafast timescale using TRED. The limitation in time resolution of both TRED and TRXD can be overcome with the advent of XFELs. Sub-100 fs X-ray pulses generated from XFELs will allow us to achieve a superb time resolution in the TRXD measurements of reaction dynamics. In addition, high photon flux and high coherence of the XFEL-generated pulses will be able to readily probe quantum-mechanical coherent phenomena such as nuclear wave packet motions. In the following sections we will discuss the potential applications of XFELs in studying reaction dynamics.

3. Photochemistry in the gas phase

The gas phase is an ideal place for examining reaction dynamics owing to its isolated collision-free environment. Accordingly, there have been many studies of reaction dynamics in the gas phase using optical spectroscopy (Zewail, 1994) and time-resolved electron diffraction (Williamson *et al.*, 1997; Ihee *et al.*, 2001; Ruan *et al.*, 2001; Reckenthaeler *et al.*, 2009). In particular, time-resolved electron diffraction has been effective in probing direct structural dynamics of small molecules in the gas phase. However, the technique has been hampered in resolving ultrafast dynamics owing to the relatively poor time resolution imposed by the electron pulse duration of the order of 1 ps. The TRXD technique can complement this limitation when combined with a novel XFEL source.

Here, it should be noted that the X-ray diffraction technique has never been applied to study gas-phase reaction dynamics. The lack of gas-phase studies using X-ray diffraction can be mainly attributed to (i) low density of sample provided by molecular beam that is conventionally used for gas-phase reaction dynamics studies and (ii) low flux of X-ray pulses from synchrotron sources. However, from the advance of the gas-phase ultrafast electron diffraction technique, it has already been demonstrated that a gas pressure sufficient for X-ray diffraction measurements using XFELs can be achieved using a medium-pressure nozzle. Let us consider that the number of electrons per pulse used in a typical time-resolved electron diffraction is $\sim 10^4$ at 1 kHz repetition rate (Ihee *et al.*, 2001). Then, in order to make up for the deficiency in the scattering intensity (1×10^6) and the repetition rate ($\sim$100 Hz for XFELs), one would need 10^{11} ($= 10^4 \times 10^6 \times 10$) X-ray photons per pulse. Since XFELs can generate X-ray pulses containing 10^{12} photons per pulse, gas-phase structural dynamics can be easily probed by TRXD under similar conditions as for TRED (with a sample pressure of 1–10 torr in the diffraction volume). Besides, the TRXD using XFELs will have a time resolution limited by the X-ray pulse duration of $\sim$100 fs, which is not only ten times better than state-of-the-art electron diffraction but also comparable with the period of molecular vibrations. With such a time resolution, the movement of atoms in a molecule can be recorded literally in 'real time'. Thus, X-ray diffraction using XFELs will open a new horizon in gas-phase reaction dynamics.

For the first gas-phase TRXD experiment, the molecules of interest include diatomic molecules, for example, I_2 and NaI. Previously, photodissociation dynamics of these small molecules have been intensely studied in the gas phase using femtosecond optical spectroscopy and ultrafast electron diffraction. Furthermore, the electron diffraction signals in the femtosecond regime have already been simulated for some of these systems (Williamson & Zewail, 1994; Geiser & Weber, 1998). Owing to vast amounts of both experimental and theoretical results available for comparison and accessibility by quantum chemistry owing to their simple molecular structure, these molecules are ideal systems to test the performance of femtosecond X-ray diffraction experiments using XFELs.

To obtain a glimpse of what type of detailed information can be obtained from this novel experiment, we take a closer look at one of the proposed systems, iodine (I_2) in the gas phase. As shown in Fig. 2, once a ground-state iodine molecule is excited to a strongly bound B state and then relaxes to a repulsive $^1\Pi$ state, the distance between the two atoms will increase and the iodine molecule will eventually dissociate into two iodine atoms. By making use of sub-100 fs time resolution and the highly coherent nature of the X-ray pulses generated from XFELs, many important aspects of this photodissociation reaction, other than a simple reaction rate, can be elucidated.

First of all, the initial dynamics of the wave packet motion in the excited state, which cannot be resolved by picosecond X-ray or electron diffraction, can be directly probed by XFELs. When an iodine molecule is photoexcited by an ultrashort laser pulse, a rovibrational wave packet is coherently prepared on the B state. As the wave packet evolves in the bound B state, the motions of the wave packet will result in oscillations of I—I bond length and orientation of the iodine molecule. Such oscillation in molecular structure and orien-

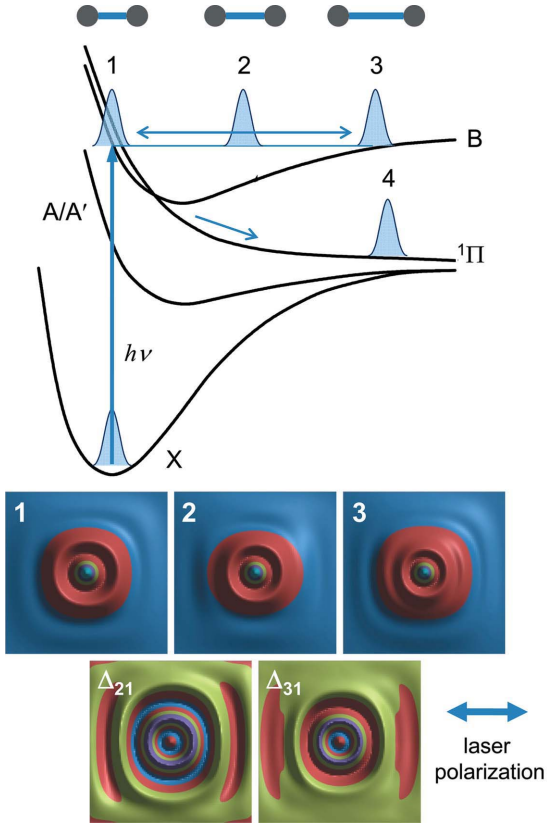

Figure 2
Photodissociation dynamics of iodine (I_2) in the gas phase. Once the iodine molecule is photoexcited to a bound *B* state by a linearly polarized coherent laser pulse, the coherently prepared rovibrational wave packet evolves in the *B* state, inducing oscillation of the I—I bond length (1, 2 and 3) and molecular orientation. The oscillation in the bond length is manifested in the X-ray diffraction patterns, as shown at the bottom. The difference diffraction patterns (Δ_{21} and Δ_{31}) between the images obtained at different nuclear configurations reflect the changes in molecular structure associated with wave packet motions. In addition, the anisotropy in the diffraction pattern is distinct owing to the alignment of molecular orientation along the laser polarization direction. The ability to transiently align the molecule using polarized excitation will freeze the orientation of the molecule, allowing us to determine the molecular structure more accurately in an aligned molecule. As time evolves after photoexcitation, the excited population will be transferred to a repulsive $^1\Pi$ state at the surface crossing between *B* and $^1\Pi$ states, leading to photodissociation to two iodine atoms (4).

tation will be manifested as a periodic change of X-ray diffraction pattern in time, giving direct evidence of quantum mechanical wave packet dynamics and related structural changes. Here, we note that the 'wave packet' term is used loosely to describe both coherent states and incoherent ensembles of iodine.

The vibrational wave packet dynamics reflected in the X-ray diffraction pattern are well demonstrated in the simulated X-ray diffraction patterns shown in Fig. 2. The two-dimensional diffraction pattern was calculated using a typical approach based on the Debye formalism. Here, we note that, to simplify the calculation, we used the Debye formalism that takes into account only the interatomic distance of constituent atoms based on the Born–Oppenheimer approximation. In principle, however, X-ray diffraction patterns are sensitive to the electron density distribution within a molecule rather than nuclear positions. Therefore, one may explore changes in electron density distribution by including a quantum mechanical description of molecular wavefunctions. To account for the effect of linearly polarized excitation, instead of orientationally averaging equally over θ and φ, we applied the excitation probability proportional to $\cos^2\theta$, where θ is the angle between the laser polarization and the direction of the I—I bond. A number of randomly oriented I_2 molecules were generated and treated to be excited following the $\cos^2\theta$ excitation probability. Diffraction patterns from I_2 molecules of various orientations were averaged to obtain an orientationally averaged two-dimensional diffraction pattern, as shown in Fig. 2. The X-ray diffraction patterns shown in Fig. 2 were obtained at different nuclear configurations of photoexcited iodine molecule in the bound *B* state. As the bond length between iodine atoms varies in the *B* state, it can be clearly seen that the shape and pattern of two-dimensional diffraction images change. The same wave packet motions are manifested in the femtosecond optical spectroscopic signals as vibrational and rotational quantum beats owing to quantum interference effects (Bowman *et al.*, 1989; Dantus *et al.*, 1990; Willberg *et al.*, 1991). Direct observation of these nuclear wave packet motions will aid in revealing the geometry and anharmonicity of the molecular potential energy surface, the transition dynamics at the surface crossings between different energy surfaces, and the detailed reaction pathway associated with molecular structure. For iodine in the gas phase, at 5 K, the period of vibrational coherence is ~300 fs with the coherence maintained longer than 40 ps, while the recurrence period of rotational coherence is ~600 ps with a dephasing time of ~50 ps (Bowman *et al.*, 1989; Dantus *et al.*, 1990). Considering the long lifetime of the *B* state (microsecond timescale) as well as the long dephasing time of the vibrational and rotational coherences compared with the femtosecond time resolution of the XFEL-TRXD experiment, many periods of wave packet motions should be readily resolved in the gas phase. Therefore, the coherent wave packet motions can be monitored by using XFEL pulses of sub-100 fs time resolution.

More information on the structural transitions of chemical reactions can be obtained by using polarized laser excitation. For example, if the excitation laser pulse is linearly polarized, the transition dipole moment of the excited molecule is transiently aligned along the direction of polarization, as exhibited by the anisotropic diffraction pattern in the photodissociation of $C_2F_4I_2$ (Reckenthaeler *et al.*, 2009). The ability to freeze the molecular alignment transiently will help to determine the structure of reacting molecules more accurately. For example, the dephasing of rotational coherence commonly takes tens of picoseconds, and therefore the dynamics of the vibrational wave packet occurring on hundreds of femtoseconds can be obtained from the aligned molecules. This prediction is well exhibited in the simulated X-ray diffraction patterns shown in Fig. 2. The X-ray patterns were calculated assuming that the iodine molecule is photoexcited by linearly polarized light. In the difference signals between the diffraction patterns obtained at different nuclear configurations in

the *B* state, the anisotropy along the polarization direction is distinct. Such anisotropy associated with the transient molecular alignment will persist much longer than the period of vibrational wave packet motions. Also, by monitoring the decay of such anisotropic patterns, the dephasing dynamics of the rotational wave packet can be obtained as well. Therefore, excitation using linearly polarized light will help us to characterize the transient structures and their dynamics more accurately.

For the convenience of data analysis, the measured two-dimensional diffraction image can be reduced to a one-dimensional diffraction curve by azimuthally integrating the two-dimensional image along the perimeter of the circular diffraction pattern, as was done in the data analysis of the 100 ps X-ray solution scattering experiment (Ihee *et al.*, 2005*a*; Ihee, 2009; Kim *et al.*, 2009). To examine the effect of data reduction on the anisotropic two-dimensional diffraction pattern arising from linearly polarized excitation, we compared two one-dimensional diffraction curves, one obtained with linearly polarized excitation and the other with unpolarized photoexcitation, as shown in Fig. 3. The two one-dimensional curves are identical although their two-dimensional patterns are different. Therefore, it is clear that the dimensionality reduction to the one-dimensional diffraction curve simplifies and facilitates the analysis of the measured dynamics at the sacrifice of the anisotropic information exhibited in the two-dimensional diffraction pattern.

More challenging targets for femtosecond TRXD experiments are polyatomic molecules consisting of more than two atoms. They include haloalkane molecules such as CF_3I, CF_2I_2 and $C_2F_4I_2$; organometallic compounds such as $Fe(CO)_5$ and $(C_5H_5)Co(CO)_2$; and hydrocarbons such as pyridine (C_5H_5N) and cyclohexadiene (C_6H_8). From previous works using electron diffraction, it has been shown that gas pressures sufficient for the gas-phase diffraction experiment can be easily achieved for these molecules. However, owing to the relatively poor time resolution of electron diffraction, limited to a few picoseconds, only the molecular structures of transient intermediates were obtained with the real-time movement of atoms not being captured. For example, picosecond electron diffraction studies on ring-shaped molecules such as pyridine (Lobastov *et al.*, 2001) and cyclohexadiene (Dudek & Weber, 2001) demonstrated the kinetics of the ring opening upon photoexcitation, but could not determine its detailed mechanism, *e.g.* whether the ring is broken in a symmetric or asymmetric fashion. Using the femtosecond TRXD technique, such initial atomic motions along the reaction coordinates can be captured in real time. Clusters of atoms or molecules are even more challenging. These systems have been studied by time-resolved electron diffraction (Dibble & Bartell, 1992), but only with microsecond time resolution determined by the flight time after a nozzle. Femtosecond TRXD should be able to follow the phase transition within a cluster as well, elucidating the relationship between the structural parameters and the phase transition.

To summarize, femtosecond TRXD measurement of reaction dynamics in the gas phase is feasible when considering the

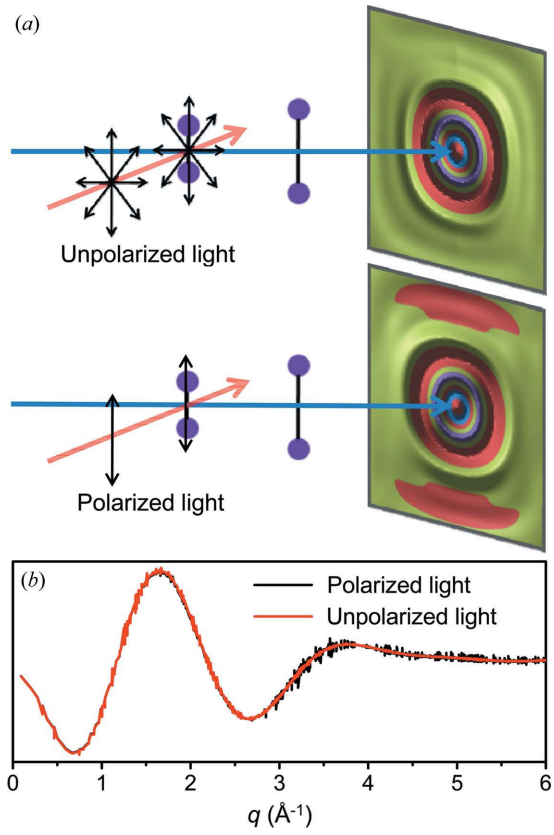

Figure 3
(*a*) The two-dimensional X-ray diffraction images are obtained after photoexcitation of an iodine molecule by either unpolarized (upper) or linearly polarized (lower) laser light. In the case of polarized excitation, the anisotropy is distinct along the direction of polarization, while no anisotropy is observed with unpolarized excitation. (*b*) Comparison of one-dimensional diffraction curves obtained by ring-integrating the two two-dimensional images shown in (*a*) along the perimeter. The one-dimensional diffraction curves obtained with linearly polarized (black) and unpolarized (red) photoexcitation are identical, indicating that the reduction of dimensionality to a one-dimensional curve will simplify and facilitate the analysis of measured dynamics at the sacrifice of the anisotropic information.

photon-counting statistics. Since the diffraction signals from the gas-phase reactions are supposed to be much simpler than those from solution reactions, which are complicated by contributions of solvent molecules, studying gas-phase reactions prior to or at least in parallel with liquid-phase reactions will be advantageous for testing the performance of the femtosecond X-ray scattering experiment using XFELs. The proposed femtosecond TRXD experiments in the gas phase will monitor the reaction dynamics in the collision-free limit and demonstrate the full power of the TRXD technique combined with XFEL sources.

The experimental set-up of gas-phase TRXD is schematically shown in Fig. 4. A femtosecond laser pulse initiates the reaction and a femtosecond XFEL pulse is subsequently sent to the sample to probe the structural dynamics. The diffraction pattern is recorded on a two-dimensional area detector. To minimize the mismatch in space and time between the pump and the probe pulses, the laser and X-ray beams are geometrically collinear. The gas vapor can be supplied through a

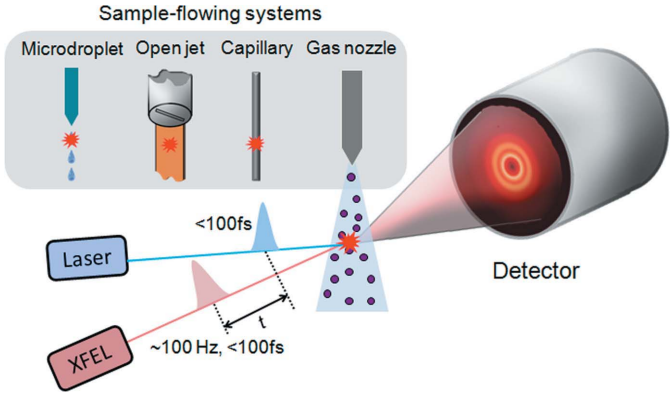

Figure 4
Schematic of the experimental set-up for time-resolved X-ray diffraction. An optical laser pulse initiates the chemical reaction in the molecules supplied by one of the sample-flowing systems, depending on the phase of the sample. Subsequently, a time-delayed X-ray pulse synchronized with the laser pulse probes the structural dynamics of the reaction. The diffracted signal is detected by a two-dimensional CCD detector to record the diffraction pattern.

medium-pressure nozzle connected to a heated sample reservoir (Ihee *et al.*, 2001). Typically, the pressure at the nozzle is about 5 torr when the backing pressure is about 100 torr. At this condition, the ambient pressure inside the vacuum chamber can be as high as 10^{-3} torr. To maintain a good vacuum in adjacent chambers, differential pumping should be employed. For both electron and X-ray diffraction experiments, the carrier gas that is normally used in time-resolved spectroscopic experiments is not desirable because the carrier gas also contributes to the diffraction, thereby increasing the background and deteriorating the signal-to-noise ratio. However, a carrier gas of low-Z value such as helium can still be used because of its relatively low scattering intensity *versus* atoms with higher Z. Clusters of atoms or molecules can be obtained as well by using a sufficiently high backing pressure.

4. Photochemistry in the liquid and solution phases

The chemistry in the solution and liquid phases has formed an important field of research because many biological and industrially important chemical reactions occur in solution. The major challenge in understanding solution-phase chemistry arises from the presence of numerous solvent molecules surrounding a solute molecule, leading to solute–solvent interactions. The solute–solvent interaction often alters the rates, pathways and branching ratios of chemical reactions through the cage effect (Hynes, 1994; Frauenfelder & Wolynes, 1985; Maroncelli *et al.*, 1989; Bagchi & Chandra, 1991; Weaver, 1992). For example, the timescale of the response of solvent molecules to electronic rearrangement of solute molecules critically affects the rates of photochemical reactions in liquid phase. Therefore, to have a better understanding of solution-phase chemical dynamics, it is crucial to consider the complex influence of the solvent medium on the reaction energetics and dynamics, *i.e.* the solvation effect.

It has been demonstrated that the solvent reorganization response to a change in solute charge distribution is strongly bimodal, that is, an initial ultrafast response owing to inertial motions followed by a slow response owing to diffusive motions (Impey *et al.*, 1982; Maroncelli & Fleming, 1988; Jimenez *et al.*, 1994). The timescale of the former is of the order of tens to hundreds of femtoseconds so, to resolve such fast dynamics, it is required to have an experimental tool with sufficient time resolution. In that regard, ultrafast laser spectroscopy in the optical and infrared regime has flourished in studying reaction dynamics in solution phase owing to their superb time resolution. While optical spectroscopies are highly sensitive to specific electronic or vibrational states, they are unable to provide information on global molecular structure. In contrast, time-resolved X-ray scattering (or diffraction) techniques can provide rather direct information on the global structure of reacting molecules, complementing the optical spectroscopy.

In recent years, we have witnessed that synchrotron-based TRXD can serve as an excellent tool for studying elementary chemical reactions in liquid and solution. For example, structural dynamics and transient intermediates in solution reactions of small molecules and proteins have been elucidated with a time resolution of 100 ps (Plech *et al.*, 2004; Bratos *et al.*, 2004; Davidsson *et al.*, 2005; Ihee *et al.*, 2005*a*; Wulff *et al.*, 2006; Kim *et al.*, 2006, 2009; Lee *et al.*, 2008; Cammarata *et al.*, 2008; Ihee, 2009). However, owing to the limited time resolution, TRXD has been only used for probing rather slow processes leading to intermediates in quasi-equilibrium, with ultrafast dynamics arising from the interplay between the solute and solvent beyond its scope. Now that highly coherent, sub-100 fs X-ray pulses are available for use with the advent of XFELs, TRXD can reach the realm of optical spectroscopy in its capability of resolving ultrafast processes. Thus, femtosecond resolution brought by the XFEL should allow investigation of ultrafast reaction dynamics in the presence of solvent interaction.

Among the candidates for the first femtosecond solution-phase TRXD experiment are diatomic molecules (I_2 and Br_2), hydrocarbons (stilbene), haloalkanes (CBr_4, CHI_3, CH_2I_2, $C_2H_4I_2$ and $C_2F_4I_2$), organometallic compounds [Platinum Pop, ferrocene, $Fe(CO)_5$, $Ru_3(CO)_{12}$ and $Os_3(CO)_{12}$] and protein molecules (myoglobin, hemoglobin and cytochrome *c*), which have been studied previously by using time-resolved X-ray diffraction with 100 ps time resolution. In particular, molecules containing heavy atoms will be promising since heavy atoms give a large signal and thus a good contrast of the solute signal against solvent background. In that regard, iodine (I_2) in solution is a good example for XFEL-based time-resolved X-ray diffraction experiments. The photodissociation and recombination of iodine in solution has been regarded as a prototype example for the solvent cage effect and thus has been a topic of intense studies (Meadows & Noyes, 1960; Harris *et al.*, 1988; Yan *et al.*, 1992; Scherer *et al.*, 1993). As shown in Fig. 5, once an iodine molecule is excited to a bound B state and relaxes to a repulsive $^1\Pi$ state, the two iodine atoms start to separate as in the gas phase. However,

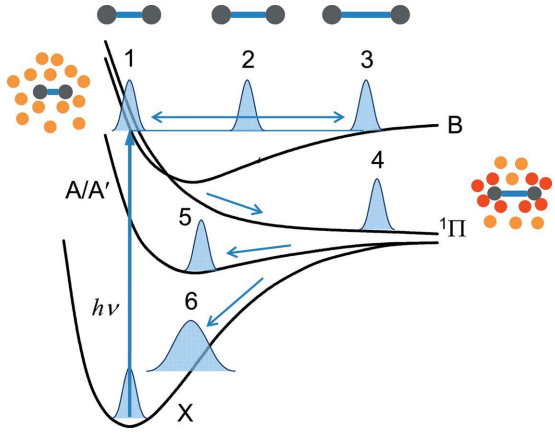

Figure 5
Photodissociation dynamics of the I_2 molecule in the solution phase. Once an iodine molecule is excited to a bound *B* state, a coherently prepared rovibrational wave packet evolves to induce the oscillation in I—I bond length (1, 2 and 3) and molecular orientation. Owing to the solute–solvent interaction, the vibrational and rotational coherences dephase much faster than in the gas phase. Once it relaxes to a repulsive $^1\Pi$ state, the internuclear distance between two iodine atoms starts to increase (4). However, owing to the cage effect by the surrounding solvent molecules, most of the excited iodine molecules geminately recombine to form a wave packet either in the *A*/*A*′ state (5) or in the hot ground state (6). These wave packet motions and transitions between energy surfaces of different states can be readily probed by femtosecond X-ray diffraction measurement.

the excited iodine molecule is soon hit by surrounding solvent molecules unlike in the gas phase. As a result, most of the excited iodine molecules geminately recombine to form a wave packet either in the hot ground state or in the *A*/*A*′ state. Previously, by using TRXD with 100 ps time resolution, rather slow relaxation of the *A*/*A*′ state to the ground state was captured, but vibrational relaxation in the hot ground state and the *A*/*A*′ state was barely resolved (Wulff *et al.*, 2006). By using femtosecond X-ray pulses from XFELs, the vibrational relaxation process that induces the rearrangement of surrounding solvent molecules can be readily resolved, accounting for the solute–solvent interaction.

Furthermore, even faster processes can be resolved by the sub-100 fs resolution of XFELs, including vibrational and rotational wave packet motions on the bound *B* state potential energy surface and curve-crossing to a dissociative state. For example, the periods of vibrational wave packet motions of iodine in hexane observed at room temperature are 160 fs and 300 fs for coherences in the ground and *B* states, respectively (Scherer *et al.*, 1993); therefore they can be easily resolved by the sub-100 fs time resolution of XFELs. The observation of such wave packet dynamics and related structural changes will give insight to the geometry of potential energy surfaces, the curve-crossing dynamics, and solvent effect on the reaction dynamics (in comparison with the experiment on iodine in the gas phase, as described in the previous section). However, owing to solute–solvent interactions, the coherent rovibrational wave packet of iodine in the solution phase dephases much faster than in the gas phase. For example, the dephasing time of a vibrational mode of $\sim$100 cm^{-1} frequency (300 fs period) in the excited *B* state is only $\sim$300 fs, limiting the visibility of oscillatory wave packet motions to only a few periods.

Another interesting topic in solution chemistry that can be studied by XFEL-TRXD is solvation dynamics. As an example, a dye molecule in solution can be considered. When a femtosecond laser pulse initiates an electronic transition of a dye molecule (*e.g.* Coumarin 153) dissolved in a polar solvent (*e.g.* methanol), a large dipole is induced in the excited-state (S_1) solute molecule in contrast to the ground state (S_0) one with zero dipole moment (Fig. 6*a*). Since this electronic transition is rapid compared with nuclear motions of the solvent molecules, the initial solvation environment is characteristic of the equilibrium condition of S_0, not of S_1. As time evolves, the surrounding solvent molecules reorganize in response to the change in charge distribution of the solute molecule in order to lower the solvation energy in the excited

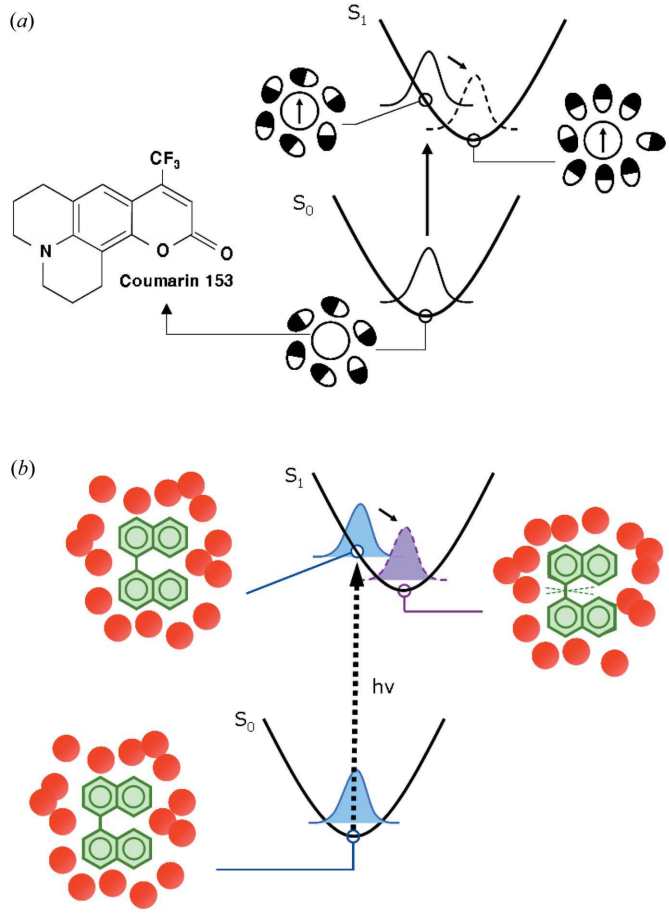

Figure 6
(*a*) Solvation dynamics of photoexcited Coumarin 153 (C153) in a polar solvent. When a C153 molecule is photoexcited to the first excited state (S_1), a large dipole is induced. As time evolves, the surrounding solvent molecules collectively reorganize in response to the change in charge distribution of the solute molecule. Such solvation response is on an ultrafast timescale and can be probed by femtosecond X-ray diffraction. (*b*) Photoisomerization of 1,1′-binaphthyl. When the ground-state (S_0) molecule is photoexcited to the first excited singlet state (S_1), the angle between two naphthyl groups is changed, resulting in reorganization of the surrounding solvent molecules. The isomerization process on the ultrafast timescale can be probed by femtosecond X-ray diffraction as well.

state. Previously, this collective motion of solvent molecules has been probed rather indirectly using optical spectroscopic methods such as fluorescence dynamic Stokes shift, photon echo and optical Kerr effect techniques (Maroncelli *et al.*, 1989; Fleming & Cho, 1996; Stratt & Maroncelli, 1996; Park *et al.*, 2003). In contrast, X-ray diffraction is able to give more direct structural information by the change in the X-ray diffraction pattern arising from the collective motion of the solvent molecules. Since these solvation dynamics have been reported to occur on an ultrafast timescale, femtosecond X-ray diffraction will be a perfect fit for characterizing this process. Another interesting subject to be studied is photoisomerization in solution (Fig. 6*b*). Photoinitiated isomerization has attracted much interest in both chemistry and biology as a candidate for photoswitching and optical memory applications (Yager & Barrett, 2006; Kawata & Kawata, 2000) and as a phototrigger for biologically relevant processes (Perman *et al.*, 1998; Gai *et al.*, 1998). As a simple example of study, we can consider the photoisomerization of 1,1′-binaphthyl. Upon photoexcitation of 1,1′-binaphthyl from the ground (S_0) to the first excited singlet state (S_1), it was proposed that the angle between the two naphthyl groups is changed by about 40° (Millar & Eisenthal, 1985). Since the surrounding solvent molecules have to be pushed out in the process, the time taken for this process is tens of picoseconds with the rate depending on the viscosity of the solvent. The femtosecond time resolution of XFELs should be sufficient to follow such fast kinetics in real time.

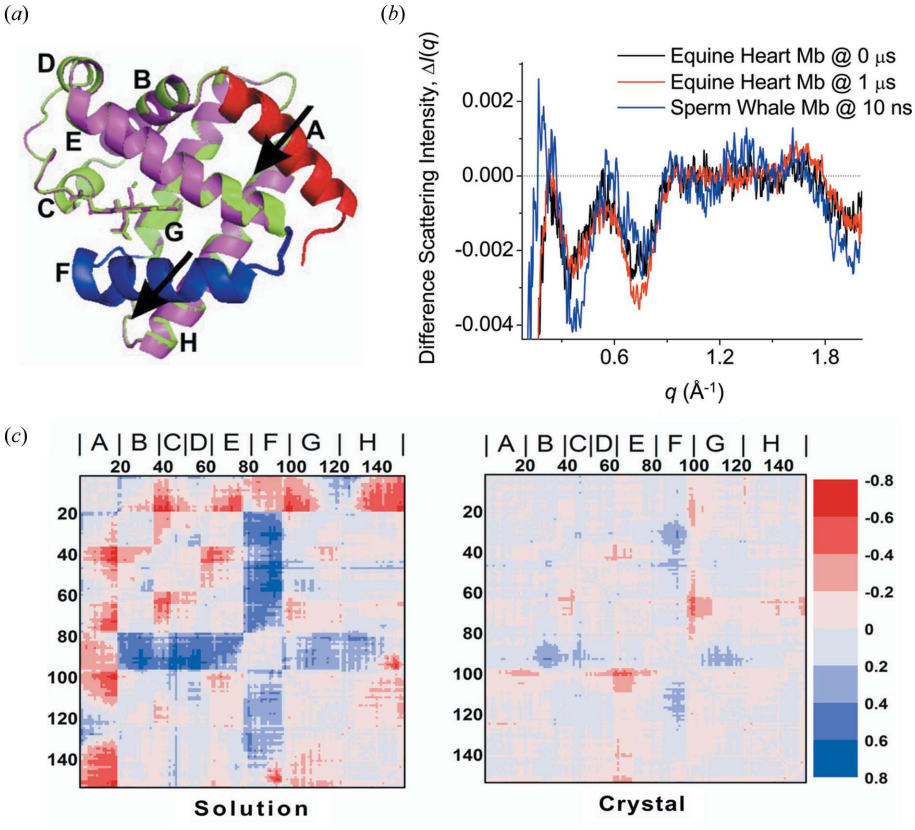

Figure 7
(*a*) The three-dimensional structure of myoglobin (Mb). (*b*) Difference scattering intensities obtained from Mbs. The wide-angle X-ray scattering (WAXS) pattern was measured for two different types of myoglobins, equine heart and sperm whale Mbs. The sperm whale Mb data were collected at a 10 ns pump–probe time delay, while equine heart Mb data were collected at 0 μs and 1 μs time delays. For the three curves, the intensity ratios of the first two negative peaks around 0.4 Å^{-1} and 0.7 Å^{-1} are different from each other. In equine heart Mb, the difference between the two data indicates the structural change between 0 and 1 μs. The sperm whale and equine heart Mbs have very similar structures with a root-mean-square deviation smaller than 0.3 Å^{-1}, but the difference signal for the two Mbs exhibit significant difference, especially in the negative peaks at 0.4 Å^{-1} and 0.7 Å^{-1}. (*c*) Difference distance maps between the structures of Mb and MbCO in solution (left) and in crystal form (right). Adapted from Ahn *et al.* (2009).

Another candidate for XFEL-TRXD experiments in the solution phase is proteins. Although they are much more challenging systems to study owing to their structural complexity compared with small molecules, the reward will be much bigger considering the immense interest in structural biology. Previously, structural dynamics of proteins including hemoglobin, myoglobin and cytochrome *c* have been studied using 100 ps X-ray solution diffraction techniques (Cammarata *et al.*, 2008; Ahn *et al.*, 2009). As an example of such an investigation, the TRXD signals of myoglobin (Mb) for two different types of Mb are shown in Fig. 7. From the difference spectra of two different species, it is clear that structural changes occur in the measured timescale. It is interesting to observe that two different types of Mb give different scattering patterns. Since the root-mean-square deviations between the two are less than 0.3 Å, this result underscores the high sensitivity of the scattering data to subtle structural differences. The improved time resolution of TRXD using XFELs will enable the elucidation of more details of the ultrafast dynamics of protein structural transitions.

As suggested in a previous section with examples of cyclohexadiene and pyridine, in the gas phase chemical reactions of organic molecules not containing any heavy-atom element can be readily studied owing to the solvent-free nature of the gas-phase environment. However, it remains quite challenging to study the reactions of such molecules in the solution phase because of low contrast of the solute signal against the solvent response and thus poor signal-to-noise ratio (SNR). The problem of low SNR might be circumvented by labeling the solute molecule with heavy atoms at the risk of modifying the structure and dynamics of the solute. Alternatively, a solvent containing much heavier atoms than the solute can be used so that a collective structural change in the solvent environment can reflect the reaction dynamics of the less visible solute molecules.

The same set-up as for the gas-phase TRXD experiments will be used for experiments for liquid and solution phases, except the sample-flowing system. For the sample-flowing system, three different set-ups can be used: a capillary, an open-jet system and a micro-droplet (see Fig. 4). In the capillary, the solution is circulated through a quartz capillary (<0.3 mm diameter) to provide a stable flow. In the open-jet system, the capillary is removed and a stable jet is produced by a high-pressure slit nozzle (<0.3 mm size) at a speed ensuring the refreshment of probe volume for every laser pulse. In the micro-droplet, drops of solution in a miniscule quantity can be provided synchronized with laser and X-ray pulses. The open-jet and micro-droplet systems have the advantage over the capillary system in that the scattering from the capillary material is absent, with substantially reduced background scattering and thus increased signal-to-noise ratio. The lower background also increases the accuracy of the normalization process. Furthermore, if the whole setting can be housed in a helium or vacuum chamber, the background from the air can be greatly reduced.

5. Single-pulse single-molecule diffraction

The high photon flux of X-ray pulses from XFELs, reaching up to 10^{12} photons per pulse, will pave the way for a novel X-ray scattering experiment: a single-pulse diffraction experiment, whereby only a single-shot image is recorded to capture the snapshots of reaction dynamics. The single-pulse diffraction experiment will not only increase the data acquisition rate substantially but will also alleviate the problem of sample deterioration by strong X-ray radiation, especially for fragile and precious protein samples. In addition, the problem of the timing jitter between the optical laser pulse and the X-ray pulse can be eliminated if each single pair of the laser and X-ray pulses can be time-stamped. In the TRXD set-up using a third-generation synchrotron, a single diffraction image is obtained by averaging the diffraction signals from 5×10^3 X-ray pulses corresponding to a total of 5×10^{12} X-ray photons. Considering a photon flux of the order of 1×10^{12} of the X-ray pulse generated from XFELs, a single shot of the XFEL pulse contains enough photons to generate a diffraction image comparable with an exposure for a few seconds using a third-generation synchrotron source. Also, if every single image can be recorded with a time index at the frequency of the macro-bunch train, *i.e.* time-stamped, the images can be sorted in time bins and averaged to improve the SNR. Therefore, the single-pulse diffraction experiment is feasible with high-photon-flux XFEL pulses.

As long as the single-pulse diffraction experiment works with a good SNR sufficient for data analysis, we can imagine a more challenging experiment, *i.e.* a single-pulse single-molecule X-ray diffraction experiment. Single-molecule X-ray diffraction using ultrashort X-ray pulses has been proposed from the early stage of XFEL development, with the prospect of overcoming the sample damage problem caused by strong X-ray radiation faced in the conventional X-ray diffraction measurements and solving the three-dimensional structure of biological macromolecules without needing to grow well diffracting single crystals (Neutze *et al.*, 2000; Hajdu, 2000; Webster & Hilgenfeld, 2002). The challenge in the single-molecule diffraction experiment arises from the poor SNR of the diffraction signal from only a single molecule as well as difficulty in handling samples of extremely low concentration. These obstacles are expected to be overcome with the aid of advanced numerical data processing procedures and electro-spraying sample injection methods, making the single-molecule diffraction experiment feasible.

The signal amplitude of single-molecule diffraction can be further enhanced if a molecule of interest, *e.g.* protein, can be labeled in a site-specific manner by using a heavy-atom probe that can scatter X-rays much more strongly. For example, it was recently demonstrated that gold nanocrystals can be used as a sensitive heavy-atom probe for measuring the length and structural fluctuations of DNA double helix (Mathew-Fenn *et al.*, 2008). By using the nanocrystal labeling scheme, the single-molecule TRXD measurement can complement single-molecule spectroscopy because it directly monitors rapid structural fluctuations of single molecules and enables direct construction of the structural conformation space.

Once the single-molecule diffraction experiment is realised, besides the structural analysis of the biological macromolecules, it will have significant implications for the study of chemical reaction dynamics. For example, we can expect to determine the structures of transition states in a chemical reaction as well as nuclear wavefunctions. Transition states connecting the reactant to the product govern the reaction rates and pathways, but their structure has never been directly characterized owing to their extremely low population and probability. For the same reason, nuclear wavefunctions of even a simple diatomic molecule have never been directly measured. Since a single-molecule diffraction pattern is determined by the structure and conformation of a single molecule, we can construct an image space consisting of single-molecule diffraction images from all possible structures and orientations of a given small molecule. Once such an image space is built, a series of measured single-molecule diffraction images can be compared with the corresponding molecular structures to determine the molecular structure of a given image. Since the occurrence probability of a particular structure is governed by the square of a nuclear wavefunction, the nuclear wavefunction can be reconstructed by sorting out a series of single-molecule diffraction images as a function of their occurrence probability and structural parameters. In principle, single-molecule diffraction can detect the instant structure of an individual molecule, and therefore it may be possible to capture the structure of transition states.

6. Conclusion

With the advent of novel XFEL sources, the time-resolved X-ray diffraction technique is envisioned to make great strides as a tool for studying reaction dynamics with rather direct structural information. Highly coherent sub-100 fs X-ray pulses generated from XFELs can be utilized to investigate

the chemical reaction dynamics in the gas and solution phases as well as structural transition dynamics of proteins, even at a single-molecule level. In this paper we proposed several interesting examples that can be studied by XFEL-TRXD. Since the femtosecond resolution has never been achieved in the reaction dynamics studies using TRXD, we will be faced with many challenges to be overcome in terms of experimental details, theory and data analysis. When these challenges are met by the efforts of researchers in the field, the XFEL-TRXD will open a new horizon in the field of reaction dynamics as well as X-ray science.

We acknowledge Dr Michael Wulff for helpful discussions. This work was supported by Creative Research Initiatives (Center for Time-Resolved Diffraction) of MEST/NRF.

References

Ahn, S., Kim, K. H., Kim, Y., Kim, J. & Ihee, H. (2009). *J. Phys. Chem. B*, **113**, 13131–13133.

Bagchi, B. & Chandra, A. (1991). *Adv. Chem. Phys.* **80**, 1–126.

Bargheer, M., Zhavoronkov, N., Woerner, M. & Elsaesser, T. (2006). *Chem. Phys. Chem.* **7**, 783–792.

Baum, P., Yang, D.-S. & Zewail, A. H. (2007). *Science*, **318**, 788–792.

Bowman, R. M., Dantus, M. & Zewail, A. H. (1989). *Chem. Phys. Lett.* **161**, 297–302.

Bratos, S., Mirloup, F., Vuilleumier, R., Wulff, M. & Plech, A. (2004). *Chem. Phys.* **304**, 245–251.

Cammarata, M., Levantino, M., Schotte, F., Anfinrud, P. A., Ewald, F., Choi, J., Cupane, A., Wulff, M. & Ihee, H. (2008). *Nat. Methods*, **5**, 881–886.

Cao, J., Hao, Z., Park, H., Tao, C., Kau, D. & Blaszczyk, L. (2003). *Appl. Phys. Lett.* **83**, 1044.

Cavalleri, A., Rini, M., Chong, H. H. W., Fourmaux, S., Glover, T. E., Heimann, P. A., Kieffer, J. C. & Schoenlein, R. W. (2005). *Phys. Rev. Lett.* **95**, 067405.

Cavalleri, A., Wall, S., Simpson, C., Statz, E., Ward, D. W., Nelson, K. A., Rini, M. & Schoenlein, R. W. (2006). *Nature (London)*, **442**, 664–666.

Chandler, D. W. & Houston, P. L. (1987). *J. Chem. Phys.* **87**, 1445–1447.

Chergui, M. & Zewail, A. H. (2009). *Chem. Phys. Chem.* **10**, 28–43.

Christensen, M., Haldrup, K., Bechgaard, K., Feidenhans'l, R., Kong, Q. Y., Cammarata, M., Lo Russo, M., Wulff, M., Harrit, N. & Nielsen, M. M. (2009). *J. Am. Chem. Soc.* **131**, 502–508.

Collet, E., Lemee-Cailleau, M.-H., Buron-Le Cointe, M., Cailleau, H., Wulff, M., Luty, T., Koshihara, S.-Y., Meyer, M., Toupet, L., Rabiller, P. & Techert, S. (2003). *Science*, **300**, 612–615.

Coppens, P., Gerlits, O., Vorontsov, I. I., Kovalevsky, A. Y., Chen, Y.-S., Graber, T. & Novozhilova, I. V. (2004). *Chem. Commun.* pp. 2144–2145.

Dantus, M., Bowman, R. M. & Zewail, A. H. (1990). *Nature (London)*, **343**, 737–739.

Davidsson, J., Poulsen, J., Cammarata, M., Georgiou, P., Wouts, R., Katona, G., Jacobson, F., Plech, A., Wulff, M., Nyman, G. & Neutze, R. (2005). *Phys. Rev. Lett.* **94**, 245503.

Dibble, T. S. & Bartell, L. S. (1992). *J. Phys. Chem.* **96**, 8603–8610.

Dudek, R. C. & Weber, P. M. (2001). *J. Phys. Chem. A*, **105**, 4167–4171.

Fleming, G. R. (1986). *Annu. Rev. Phys. Chem.* **37**, 81–104.

Fleming, G. R. & Cho, M. (1996). *Annu. Rev. Phys. Chem.* **47**, 109–134.

Frauenfelder, H. & Wolynes, P. G. (1985). *Science*, **229**, 337–345.

Gai, F., Hasson, K. C., McDonald, J. C. & Anfinrud, P. A. (1998). *Science*, **279**, 1886–1891.

Gedik, N., Yang, D.-S., Logvenov, G., Bozovic, I. & Zewail, A. H. (2007). *Science*, **316**, 425–429.

Geiser, J. D. & Weber, P. M. (1998). *J. Chem. Phys.* **108**, 8004–8011.

Hajdu, J. (2000). *Curr. Opin. Struct. Biol.* **10**, 569–573.

Hargittai, I. & Hargittai, M. (1988). *Stereochemical Applications of Gas-Phase Electron Diffraction.* New York: VCH.

Harris, A. L., Brown, J. K. & Harris, C. B. (1988). *Annu. Rev. Phys. Chem.* **39**, 341–366.

Heck, A. J. R. & Chandler, D. W. (1995). *Annu. Rev. Phys. Chem.* **46**, 335–372.

Hertel, I. V. & Radloff, W. (2006). *Rep. Prog. Phys.* **69**, 1897–2003.

Hynes, J. T. (1994). *Ultrafast Dynamics of Chemical Systems*, edited by J. D. Simon, pp. 345–381. Dordrecht: Kluwer.

Ihee, H. (2009). *Acc. Chem. Res.* **42**, 356–366.

Ihee, H., Goodson, B. M., Srinivasan, R., Lobastov, V. A. & Zewail, A. H. (2002). *J. Phys. Chem. A*, **106**, 4087–4103.

Ihee, H., Lobastov, V. A., Gomez, U. M., Goodson, B. M., Srinivasan, R., Ruan, C.-Y. & Zewail, A. H. (2001). *Science*, **291**, 458–462.

Ihee, H., Lorenc, M., Kim, T. K., Kong, Q. Y., Cammarata, M., Lee, J. H., Bratos, S. & Wulff, M. (2005*a*). *Science*, **309**, 1223–1227.

Ihee, H., Rajagopal, S., Srajer, V., Pahl, R., Anderson, S., Schmidt, M., Schotte, F., Anfinrud, P. A., Wulff, M. & Moffat, K. (2005*b*). *Proc. Natl. Acad. Sci. USA*, **102**, 7145–7150.

Impey, R. W., Madden, P. A. & McDonald, I. R. (1982). *Mol. Phys.* **46**, 513–539.

Jimenez, R., Fleming, G. R., Kumar, P. V. & Maroncelli, M. (1994). *Nature (London)*, **369**, 471–473.

Johnson, P. M. & Otis, C. E. (1981). *Annu. Rev. Phys. Chem.* **32**, 139–157.

Kao, Y.-T., Saxena, C., Wang, L., Sancar, A. & Zhong, D. (2005). *Proc. Natl. Acad. Sci. USA*, **102**, 16128–16132.

Kawata, S. & Kawata, Y. (2000). *Chem. Rev.* **100**, 1777–1788.

Khundkar, L. R. & Zewail, A. H. (1990). *Annu. Rev. Phys. Chem.* **41**, 15–60.

Kim, T. K., Lee, J. H., Wulff, M., Kong, Q. & Ihee, H. (2009). *Chem. Phys. Chem.* **10**, 1958–1980.

Kim, T. K., Lorenc, M., Lee, J. H., Russo, M., Kim, J., Cammarata, M., Kong, Q. Y., Noel, S., Plech, A., Wulff, M. & Ihee, H. (2006). *Proc. Natl. Acad. Sci. USA*, **103**, 9410–9415.

Kotaidis, V. & Plech, A. (2005). *Appl. Phys. Lett.* **87**, 213102.

Kukura, P., McCamant, D. W. & Mathies, R. A. (2007). *Annu. Rev. Phys. Chem.* **58**, 461–488.

Lee, J. H., Kim, J., Cammarata, M., Kong, Q., Kim, K. H., Choi, J., Kim, T. K., Wulff, M. & Ihee, H. (2008). *Angew. Chem. Int. Ed.* **47**, 1047–1050.

Lobastov, V. A., Srinivasan, R., Goodson, B. M., Ruan, C.-Y., Feenstra, J. S. & Zewail, A. H. (2001). *J. Phys. Chem. A*, **105**, 11159–11164.

Maroncelli, M. & Fleming, G. R. (1988). *J. Chem. Phys.* **89**, 5044–5069.

Maroncelli, M., MacInnis, J. & Fleming, G. R. (1989). *Science*, **243**, 1674–1681.

Mathew-Fenn, R. S., Das, R. & Harbury, P. A. B. (2008). *Science*, **322**, 446–449.

Meadows, L. F. & Noyes, R. M. (1960). *J. Am. Chem. Soc.* **82**, 1872–1876.

Millar, D. P. & Eisenthal, K. B. (1985). *J. Chem. Phys.* **83**, 5076–5083.

Neumark, D. M. (2001). *Annu. Rev. Phys. Chem.* **52**, 255–277.

Neutze, R., Wouts, R., van der Spoel, D., Weckert, E. & Hajdu, J. (2000). *Nature (London)*, **406**, 752–757.

Nibbering, E. T. J., Fidder, H. & Pines, E. (2005). *Annu. Rev. Phys. Chem.* **56**, 337–367.

Park, S., Flanders, B. N., Shang, X., Westervelt, R. A., Kim, J. & Scherer, N. F. (2003). *J. Chem. Phys.* **118**, 3917–3920.

Perman, B., Srajer, V., Ren, Z., Teng, T., Pradervand, C., Ursby, T., Bourgeois, D., Schotte, F., Wulff, M., Kort, R., Hellingwerf, K. & Moffat, K. (1998). *Science*, **279**, 1946–1950.

Pirenne, M. H. (1946). *The Diffraction of X-rays and Electrons by Free Molecules.* Cambridge: The University Press.
Plech, A., Kotaidis, V., Lorenc, M. & Boneberg, J. (2006). *Nat. Phys.* **2**, 44–47.
Plech, A., Wulff, M., Bratos, S., Mirloup, F., Vuilleumier, R., Schotte, F. & Anfinrud, P. A. (2004). *Phys. Rev. Lett.* **92**, 125505.
Qiu, W., Wang, L., Lu, W., Boechler, A., Sanders, D. A. R. & Zhong, D. (2007). *Proc. Natl. Acad. Sci. USA*, **104**, 5366–5371.
Reckenthaeler, P., Centurion, M., Fuß, W., Trushin, S. A., Krausz, F. & Fill, E. E. (2009). *Phys. Rev. Lett.* **102**, 213001.
Rischel, C., Rousse, A., Uschmann, I., Albouy, P.-A., Geindre, J.-P., Audebert, P., Gauthier, J.-C., Forster, E., Martin, J.-L. & Antonetti, A. (1997). *Nature (London)*, **390**, 490–492.
Ruan, C.-Y., Lobastov, V. A., Srinivasan, R., Goodson, B. M., Ihee, H. & Zewail, A. H. (2001). *Proc. Natl. Acad. Sci. USA*, **98**, 7117–7122.
Ruan, C.-Y., Lobastov, V. A., Vigliotti, F., Chen, S. & Zewail, A. H. (2004). *Science*, **304**, 80–84.
Scherer, N. F., Jonas, D. M. & Fleming, G. R. (1993). *J. Chem. Phys.* **99**, 153–168.
Sciaini, G., Harb, M., Kruglik, S. G., Payer, T., Hebeisen, C. T., zu Heringdorf, F. J. M., Yamaguchi, M., Horn-von Hoegen, M., Ernstorfer, R. & Miller, R. J. D. (2009). *Nature (London)*, **458**, 56–59.
Shorokhov, D., Park, S. T. & Zewail, A. H. (2005). *Chem. Phys. Chem.* **6**, 2228–2250.
Siwick, B. J., Dwyer, J. R., Jordan, R. E. & Miller, R. J. D. (2003). *Science*, **302**, 1382–1385.
Stolow, A. (2003). *Annu. Rev. Phys. Chem.* **54**, 89–119.
Stratt, R. M. & Maroncelli, M. (1996). *J. Phys. Chem.* **100**, 12981–12996.
Vorontsov, I. I., Graber, T., Kovalevsky, A. Y., Novozhilova, I. V., Gembicky, M., Chen, Y.-S. & Coppens, P. (2009). *J. Am. Chem. Soc.* **131**, 6566–6573.
Weaver, M. J. (1992). *Chem. Rev.* **92**, 463–480.
Webster, G. & Hilgenfeld, R. (2002). *Single Mol.* **3**, 63–68.
Willberg, D. M., Breen, J. J., Gutmann, M. & Zewail, A. H. (1991). *J. Phys. Chem.* **95**, 7136–7138.
Williamson, J. C., Cao, J., Ihee, H., Frey, H. & Zewail, A. H. (1997). *Nature (London)*, **386**, 159–162.
Williamson, J. C. & Zewail, A. H. (1994). *J. Phys. Chem.* **98**, 2766–2781.
Wulff, M., Bratos, S., Plech, A., Vuilleumier, R., Mirloup, F., Lorenc, M., Kong, Q. & Ihee, H. (2006). *J. Chem. Phys.* **124**, 034501.
Yager, K. G. & Barrett, C. J. (2006). *J. Photochem. Photobiol. A*, **182**, 250–261.
Yan, Y., Whitnell, R. M., Wilson, K. R. & Zewail, A. H. (1992). *Chem. Phys. Lett.* **193**, 402–412.
Yang, D.-S. & Zewail, A. H. (2009). *Proc. Natl. Acad. Sci. USA*, **106**, 4122–4126.
Zewail, A. H. (1994). *Femtochemistry: Ultrafast Dynamics of the Chemical Bond*, Vol. I and II. Singapore: World Scientific.
Zhang, L., Wang, L., Kao, Y.-T., Qiu, W., Yang, Y., Okobiah, O. & Zhong, D. (2007). *Proc. Natl. Acad. Sci. USA*, **104**, 18461–18466.